Accepted Manuscript

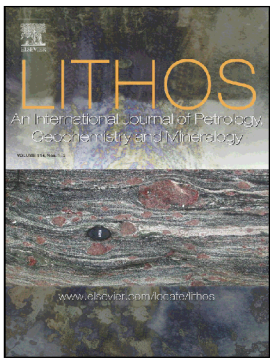

Chromium spinel in Late Quaternary volcanic rocks from Kamchatka: Implications for spatial compositional variability of subarc mantle and its oxidation state

Nikolai Nekrylov, Maxim V. Portnyagin, Vadim S. Kamenetsky, Nikita L. Mironov, Tatiana G. Churikova, Pavel Yu Plechov, Adam Abersteiner, Natalia V. Gorbach, Boris N. Gordeychik, Stepan P. Krasheninnikov, Daria P. Tobelko, Maria Yu Shur, Sofia A. Tetroeva, Anna O. Volynets, Kaj Hoernle, Gerhard Wörner

PII:	S0024-4937(18)30376-1
DOI:	doi:10.1016/j.lithos.2018.10.011
Reference:	LITHOS 4827
To appear in:	*LITHOS*
Received date:	20 July 2018
Accepted date:	12 October 2018

Please cite this article as: Nikolai Nekrylov, Maxim V. Portnyagin, Vadim S. Kamenetsky, Nikita L. Mironov, Tatiana G. Churikova, Pavel Yu Plechov, Adam Abersteiner, Natalia V. Gorbach, Boris N. Gordeychik, Stepan P. Krasheninnikov, Daria P. Tobelko, Maria Yu Shur, Sofia A. Tetroeva, Anna O. Volynets, Kaj Hoernle, Gerhard Wörner , Chromium spinel in Late Quaternary volcanic rocks from Kamchatka: Implications for spatial compositional variability of subarc mantle and its oxidation state. Lithos (2018), doi:10.1016/j.lithos.2018.10.011

Chromium spinel in Late Quaternary volcanic rocks from Kamchatka: Implications for spatial compositional variability of subarc mantle and its oxidation state

Nikolai Nekrylov[1,2,*], Maxim V. Portnyagin[3,4], Vadim S. Kamenetsky[1,5], Nikita L. Mironov[4], Tatiana G. Churikova[6,7], Pavel Yu. Plechov[2], Adam Abersteiner[5], Natalia V. Gorbach[6], Boris N. Gordeychik[1,7], Stepan P. Krasheninnikov[4], Daria P. Tobelko, Maria Yu. Shur[8], Sofia A. Tetroeva[8], Anna O. Volynets[6], Kaj Hoernle[3] and Gerhard Wörner[7]

[1] *Institute of Experimental Mineralogy RAS, 142432, Chernogolovka, Russia*

[2] *Fersman Mineralogical Museum RAS, 119071, Moscow, Russia*

[3] *GEOMAR Helmholtz Centre for Ocean Research Kiel, 24148, Germany.*

[4] *Vernadsky Institute of Geochemistry and Analytical Chemistry RAS, 119991, Moscow, Russia*

[5] *Earth Sciences and CODES, University of Tasmania, TAS 7001, Hobart, Australia*

[6] *Institute of Volcanology and Seismology FEB RAS, 683006, Petropavlovsk-Kamchatsky, Russia*

[7] *GZG, Abt. Geochemie, Göttingen Universität, 37077, Göttingen, Germany*

[8] *Lomonosov Moscow State University, Moscow, Russia*

[*] *Corresponding author (email: nekrilov.n@gmail.com)*

Abstract

The Kamchatka volcanic arc (Russia) is one of well-studied but complex tectonic margins on Earth, with an extensive geologic history stretching as far back as the Late Cretaceous. Unlike many other subduction zones, primitive basalts with Mg# > 65 are abundant in Kamchatka, thereby allowing characterization of the mantle source through compositional analyses of near-liquidus minerals in the rocks. In this paper, we present a comprehensive dataset on the composition of Cr-spinel inclusions in olivine for all main Late Quaternary volcanic zones in Kamchatka, comprising of analyses of 1604 spinel inclusions and their host-olivine from 104 samples representing 30 volcanoes and volcanic fields. The studied rocks are basalts, basaltic andesites and high-Mg andesites, which cover the whole compositional range the Late Quaternary primitive volcanic rocks in Kamchatka. The composition of spinel shows large variability. Spinel inclusions with the lowest Cr# and Fe^{3+}/Fe^{2+} ratios were found in basalts from Sredinny Range and Northern Kamchatka, whereas the most Cr-rich and oxidized spinel inclusions occur in basalts and high-Mg andesites from the Central Kamchatka Depression. Intermediate Cr-spinel compositions characterize the Eastern Volcanic Belt of Kamchatka. The compositions of olivine-spinel pairs were used to quantify the oxidation state of parental Kamchatka magmas and the degree of partial mantle melting. The redox conditions recorded in spinel compositions range from ΔQFM=+0.7 to +3.7. ΔQFM for samples from the Sredinny Range and Northern Kamchatka correlates with a number of proxies of the involvement of slab-derived components incorporated in the composition of their host-rocks (e.g., La/Nb and Ba/La), which suggests a coupling between the mantle oxidation and metasomatism by slab-derived fluids or melts. These correlations were not observed for frontal Kamchatka volcanoes with the highest estimated ΔQFM, which possibly indicates a buffering of the mantle oxidation state by sulfur. The estimated degrees of partial mantle melting range from 8 to > 20% for Kamchatka volcanoes. Spinel from the Central Kamchatka Depression has the highest Cr# and could

crystallize from magmas generated from the most depleted sources. In contrast to the Eastern Volcanic Belt, spinel Cr# and the inferred degrees of melting in the Central Kamchatka Depression do not correlate with spinel TiO_2 content. The apparent decoupling between the proxies of mantle depletion in the CKD spinel is interpreted to reflect refertilization of the CKD mantle by oxidized Ti-rich slab- or mantle lithosphere-derived melts near the northern edge of the subducting Pacific Plate. This study demonstrates that the composition of Cr-spinel in volcanic rocks in combination with bulk-rock compositions can be a powerful tool to map regional variations of the mantle source depletion, oxidation state, and involvement of various slab derived components in island-arc magmatism.

Key words: Cr-spinel, Olivine, Kamchatka, Redox conditions, Mantle wedge.

1. Introduction

Subduction-related magmatism occurs due to interaction of mantle wedge and slab-derived hydrous fluids and melts (e.g., Tatsumi and Eggins, 1995). Variations of mantle temperature, depth of melting, composition and flux of slab-derived components cause large compositional heterogeneity in the mantle wedge, which affects the composition of arc magmas and the rheological properties of the mantle (e.g., Ewart et al., 1998; Hirth and Kohlstedt, 2003; Peate et al., 1997; Su et al., 2015). Although studies addressing regional spatial and/or temporal variations of the mantle wedge composition and its oxidation state are rare (e.g., Brounce et al., 2014; Deering et al., 2010), they provide unique insights into the dynamics and evolution of arc systems.

Cr-spinel is a common accessory mineral which occurs in most types of primitive high-Mg volcanic rocks. Due to multicomponent composition, Cr-spinel is considered to be an important petrological indicator of parental magma composition, source fertility and magma

oxidation state (e.g., Irvine, 1965; Kamenetsky et al., 2001; Barnes and Roeder, 2001; Leuthold et al., 2015). Magmatic spinel is very sensitive to the composition of equilibrium melt and crystallization conditions, and therefore it can be a powerful tool for discrimination of magmatic rocks from different geodynamic settings (Arai, 1992; Barnes and Roeder, 2001; Kamenetsky et al., 2001). In combination with the compositions of other minerals (e.g., olivine), spinel can be used to quantitatively characterize mantle source depletion (e.g., Arai 1994) and conditions of crystallization, such as temperature (e.g., Ballhaus et al., 1991; Irvine, 1965;O'Neill and Wall, 1987; Wan et al., 2008) and oxygen fugacity (e.g., Ballhaus et al., 1991; Mattioli and Wood, 1988; O'Neill and Wall, 1987).

In this contribution, we examine the Kamchatka volcanic arc (Russia) located in the northwestern corner of the Pacific Ring of Fire. We present an extensive compositional dataset of spinel inclusions hosted in high-Mg olivine from mafic volcanic rocks in order to characterize the compositional variability and oxidation state of the mantle beneath Kamchatka. Our results demonstrate that subduction-related processes have a strong influence on the oxidation of subarc mantle. Furthermore, we suggest that there were large variations of the degrees of partial mantle melting, which could have been previously underestimated, based on fluid-immobile incompatible element systematics in magmas.

2. Geological setting and samples

The Kamchatka volcanic arc is located in the northwestern corner of the Pacific Ring of Fire. It is connected with the Kurile volcanic arc along its southern margin and links at a nearly right angle with the Aleutian Arc in the north. Quaternary volcanism in Kamchatka occurs in response to subduction of the Pacific oceanic plate under the Eurasian continental margin (e.g., Gorbatov et al., 1997). The Pacific plate is currently subducting under the southern and central parts of Kamchatka at a rate of ~8 cm/yr (DeMets et al., 1990). At the Kamchatka-Aleutian arc junction, the subduction trench terminates at approximately 55°N,

however, no geophysical constraints on the subducted plate have been produced for the north of Kamchatka (Levin et al., 2002). The geological history of Kamchatka extends into the Late Cretaceous and includes numerous episodes of terrain accretion, stretching and *in-situ*, subduction-related volcanism (Avdeiko et al., 2007; Lander and Shapiro, 2007). According to Lander and Shapiro (2007), Kamchatka is comprised of two major volcanic belts: i) the Eastern Kamchatka Volcanic Belt, and ii) Central Kamchatka Volcanic Belt (Fig. 1). The Wadati-Benioff zone is located at 90–200 km depth beneath the Eastern Kamchatka Volcanic Belt and at > 300 km depth under the southern part of Central Kamchatka Volcanic Belt (Gorbatov et al., 1997; Zhao et al., 2010). The Eastern Kamchatka Volcanic Belt hosts the most active volcanoes in Kamchatka and numerous volcanic fields of monogenetic cinder cones and associated lavas. The belt includes three major segments, which are distinct in age of volcanism, spatial distribution of volcanoes and rock composition: i) southern segment or South Kamchatka (SK; ~51.1^{o}–52.9^{o} N), ii) central segment or Eastern Volcanic Front (EVF; ~52.9^{o}–55.3^{o} N), and iii) northern segment, which includes volcanoes of the Central Kamchatka Depression (CKD; ~55.3–57.4^{o} N). The SK segment is the continuation of the Northern Kurile Arc and has been volcanically active since the Late Eocene. The central (EVF) and northern (CKD) segments have been established more recently, beginning from the Late Miocene (EVF) to Quaternary (CKD) (Lander and Shapiro, 2007). The central and northern segments formed in response to an echelon accretion of Shipunsky, Kronotsky and Kamchatsky (collectively called 'Eastern') Peninsulas in Kamchatka, which propagated south to north, causing the eastward migration of volcanism from the Central Kamchatka Volcanic Belt (e.g., Avdeiko et al., 2007; Lander and Shapiro, 2007; Park et al., 2002). The Central Kamchatka Volcanic Belt (Sredinny Range, SR) traverses the Sredinny mountain range and is formed by numerous historically inactive polygenetic volcanoes, monogenetic cones and related lava fields (Churikova et al., 2001; Ponomareva et al., 2007; Volynets et al., 2010). Quaternary volcanism in North Kamchatka is represented by a chain of extinct volcanoes and

fields of monogenetic cones extending from Nachikinsky volcano on Ozernoy Peninsula in the northernmost CKD towards the Sredinny Range. This volcanism is not related to modern subduction, but formed due to decompression mantle melting, possibly following slab break-off under this region (Levin et al., 2002; Portnyagin et al., 2005a, 2007a). In this work we refer to this particular region as North Kamchatka (NK).

We studied composition of Cr-spinel inclusions in olivine from 104 samples representing 30 volcanoes and volcanic fields from all main late Quaternary volcanic zones of Kamchatka (Fig. 1): SK (Bol'shaya Ipel'ka, Savan River, Asacha, Opala, Tolmachev Dol volcanic field, Tolmachev, Mutnovsky, Gorely, Barkhatnaya Sopka), EVF (Avachinsky, Zhupanovsky, Bakening, Karymsky, Schmidt, Gamchen, Komarov), CKD (Tolbachik, Kamen, Klyuchevskaya Sopka, Ploskie Sopki volcanic massif, Kharchinsky, Zarechny, Shiveluch, Shisheisky Complex), SR (Ichinsky, Akhtang, Kekuknaisky volcanic field, Sedanka volcanic field, Tobeltsen) and NK (Nachikinsky). Bulk-rock compositions for most samples were previously reported (Bindeman et al., 2005; Churikova et al., 2001, 2013; Dirksen and Melekestsev, 1999; Dorendorf et al., 2000a; Duggen et al., 2007; Gorbach et al., 2013; Gorbach and Portnyagin, 2011; Grib and Perepelov, 2008;Plechova et al., 2011; Portnyagin et al., 2005a, 2005b, 2007b, 2015; O. Volynets, 1994; O. Volynets et al., 2000; A. Volynets et al., 2010). The host rocks have MgO > 4 wt.%, Mg# > 0.46 and represent the entire range of primitive to moderately fractionated rock compositions in Kamchatka (Fig. 2). The majority of the rocks are basalts, basaltic andesites and high-Mg andesites of the medium-K subalkaline series. Low-K basalts (3 samples) are from Avachinsky and Mutnovsky volcanoes, and high-K basalts (7 samples) are from Bolshaya Ipel'ka, Tolbachik and Shiveluch volcanoes. High-K basaltic trachyandesites are from Nachikinsky volcano in NK. The bulk-rock compositions are presented in Supplementary Table 1.

3. Dataset and analytical methods

The dataset comprising of ~2000 analyses of olivine-hosted spinel inclusions and their host olivine grains was collected in several laboratories over the last 20 years. The majority of the data was obtained at GEOMAR (Kiel) using a Cameca SX50 (until 2007) and JEOL JXA8200 (2007–present) and in GZG (Geochemisches Institut, Göttingen) using a JEOL JXA 8900RL. Standardization and quality control in GEOMAR lab was carried out using common reference materials: chromite NMNH117075, ilmenite NMNH96189 and olivine NMNH111312-44 (Jarosewich et al., 1980). The analyses were performed at 15 kV accelerating voltage, 20 nA for spinels and 20, 100 or 300 nA for olivine. Typical on-peak counting time was 20s for all elements. Some recent analyses of olivine were performed at 300 nA and 100–300 s counting time for trace elements (Al, Mn, Ni, Ca, Cr). For standardization of major and trace elements in spinel and olivine, a program in GZG lab used a set of synthetic and natural standards. Peak counting times for major elements were 15–30 s. To ensure accuracy and high precision of olivine analyses and to correct for instrumental drift, we used two San Carlos olivine crystals: USNM 111312/444 (Jarosewich et al., 1980) and commercial San Carlos olivine as "in house" standard crystal SC-Goe (for details see Churikova et al., 2007; Gordeychik et al., 2018). The analyses were performed at 15–20 kV accelerating voltage, 20 nA for spinels, and 300 nA for olivine using 60-300 s counting time for trace elements (Mn, Co, Cr, Ni, Zn, Al, Ca, P) except for two olivine crystals measured at 15 kV and 15 nA using 30 s counting time for Ni.

The remaining analyses were obtained at the Vernadsky Institute, Moscow (Camebax microbeam and Cameca SX-100 operated at 15 kV, 50 nA) and at the Lomonosov State University, Moscow (EDS CamScan 4DV operated at 15 kV, 1 nA and WDS JEOL JSM-6480 operated at 15 kV, 15 nA). The laboratories are indicated in Supplementary Table 2. Additional information about the analytical techniques can be found in papers devoted to study particular volcanoes in Kamchatka: Avachinsky (Portnyagin et al., 2005b), Zhupanovsky (Plechova et al., 2011), Mutnovsky (Shishkina et al., 2018), Gorely (Nazarova

et al., 2017), Karymsky (Nazarova et al., 2019), Klyuchevskoy (Mironov et al., 2015), Shiveluch (Gorbach and Portnyagin, 2011; Gordeychik et al., 2018) and Kekuknaisky (Nekrylov et al., 2018).

The entire dataset was processed to exclude poor quality data and magnetite grains. Analyses containing more than 1 wt.% of SiO_2 were excluded due to contamination by the host olivine. Spinel inclusions, which contain more than 50 wt.% FeO, were also excluded because they represent the late stage magmatic crystallization, which is beyond the scope of this study. The final dataset consists of 1604 olivine-hosted spinel inclusions (Supplementary Table 2): 230 inclusions from 13 samples, representing 9 volcanoes and volcanic fields of SK; 261 inclusions from 17 samples, representing 7 volcanoes and volcanic fields of EVF; 904 inclusions from 58 samples, representing 8 volcanoes and volcanic fields of CKD; 159 inclusions from 13 samples, representing 5 volcanoes and volcanic fields of SR; 50 inclusions from 3 samples representing, 1 volcano of NK. A summary of the data is provided in Table 1. Fe^{2+} and Fe^{3+} in spinel were calculated on the basis of ideal spinel stoichiometry as a mixture of ulvöspinel and spinel-type components.

New bulk-rock analyses reported here were performed at the Helmholtz Centre for Ocean Research Kiel (GEOMAR) following method described by Portnyagin et al. (2015). Analyses of AVA-17-06, AVA-17-08 and SHIV-10-24 samples were performed at GZG Göttingen Universität following method described by Churikova et al. (2001).

4. Results

4.1 Composition of host olivine

Composition of olivine grains (Fo = Mg/(Mg+Fe), mol.%) hosting Cr-spinel inclusions in Kamchatka rocks varies from $Fo_{71.7}$ to $Fo_{92.5}$ (Supplementary Table 2; Fig. 3). The most Fo-rich olivine in different volcanic zones is $Fo_{86.4}$ for SK, $Fo_{91.4}$ for EVF, $Fo_{92.5}$ for CKD, $Fo_{87.1}$ for SR and $Fo_{86.5}$ for NK. Modes of Fo-number, which can be regarded as the characteristic of

average degree of magma fractionation, also vary between the zones and correlate with maximum Fo-number determined for each volcanic zone (Fig. 3): $Fo_{84–85}$ for SK, $Fo_{86–87}$ for EVF, $Fo_{88–89}$ for CKD, $Fo_{80–81}$ for SR and $Fo_{84–85}$ for NK. The least magnesian olivine has approximately the same composition (Fo_{72}) in all volcanic zones and corresponds to the appearance of Ti-magnetite, which contains more than 50 wt.% total FeO and was not included in the dataset (Fig. 4a).

4.2 Composition of Cr-spinel inclusions in olivine

The Cr# (Cr/(Cr+Al)×100, mol.%) of studied spinel inclusions varies from 1.1 to 85.1 (Figs. 4a, c). The majority of spinel inclusions from CKD samples have Cr# = 60–80, whereas only a few samples from other volcanic zones contain spinel with Cr# > 60. Spinel inclusions from SK, SR and NK have Cr# in the range of 20–60. Only spinel inclusions from EVF cover the whole range of Cr# observed in Kamchatka samples. Spinel with high Cr# = 70–80 in EVF were found in samples from the Karymsky volcano and in avachites – exotic picrobasalts from the Avachinsky volcano (Portnyagin et al., 2005b). Mg# of spinel inclusions varies from 25.0 to 76.5 mol.%, even within the narrow range of olivine Fo (Fig. 4b). This is because spinel inclusions trapped in olivine grains of narrow compositional range (e.g., $Fo_{84–86}$) exhibit negative correlations between Mg# and Cr# (Supplementary Table 3, Fig. 4d), as expected from strong dependence of the Mg-Fe olivine-spinel partitioning on spinel Cr# (e.g., Kamenetsky et al., 2001). The Mg# of spinel inclusions at given Cr# correlates positively with the Fo-number of host olivine (Fig. 4b). Cation fraction of Fe^{3+} in Kamchatka spinel increases and Fe^{2+}/Fe^{3+} ratio decreases with decreasing host olivine Fo-number (Fig. 4e) without clear distinction between different volcanic zones in Kamchatka.

5. Discussion

5.1 Composition of primitive spinel

In order to assess the composition of primitive olivine-spinel assemblage in Kamchatka rocks, which crystallized from near primary magmas, we filtered our database to exclude spinel hosted by olivine grains with $Fo_{<84}$, which are also strongly enriched in Fe and Ti and approach Ti-magnetite composition. The remaining spinel inclusions in olivine $Fo_{84–92.5}$ are present in our dataset for 27 out of 30 volcanoes from all volcanic zones in Kamchatka (449 inclusions from 79 samples). Spinel inclusions in olivine $Fo_{>84}$, which crystallized from near primary or slightly fractionated magmas, are referred thereafter as 'primitive spinel'. Significant parts of this dataset comprise compositions of spinel trapped in olivine with $Fo_{>88}$, which could crystallize from near *primary* mantle-derived magmas. However, high-Fo olivine was not found in all volcanic zones, thereby hampering comparisons with regards to spinel composition. The compositions of primitive spinel trapped by the most Mg-rich olivine from every sample were averaged and together with their host rock composition and presented in Supplementary Table 4.

Cr# in primitive spinel from Kamchatka varies from 21.0 to 79.7 (Fig. 5a), which can be caused either by fractionation of Cr-rich phases, such as high-Ca pyroxene and Cr-spinel (Smith and Leeman, 2005) or by compositional variations in parental magmas and their sources, due to variations of Cr/Al ratio (Arai, 1994; Dick and Bullen, 1984). As illustrated in Figure 5, Cr# in spinel from CKD volcanoes, where olivine phenocrysts have full range of compositions from $Fo_{92.5}$ to Fo_{72}, does not correlate systematically with the Fo-number of the host olivine. Based on this observation, we conclude that Cr# in Kamchatka spinel is not significantly affected by fractionation of pyroxene and spinel, which typically accompany olivine during the early stages of crystallization of primitive Kamchatka magmas (e.g., Bergal-Kuvikas et al., 2017; Portnyagin et al., 2015). Thus, the variations in primitive spinel Cr# between different samples and volcanic zones in Kamchatka are likely related to variability of the primary melt compositions and their mantle sources.

Direct comparison of the composition of primitive spinel inclusions and the composition of their host rocks provides additional evidence of a close relationship between them. Kamenetsky et al. (2001) showed that Al_2O_3 content in primitive spinel correlates strongly with Al_2O_3 contents in equilibrium melt. In our case, we compared Al_2O_3 content of spinels with the host rocks (Fig. 5d). Despite some scatter, a correlation is evident between Al_2O_3 content in spinel and in host rocks. The trend is comparable to that proposed by Kamenetsky et al. (2001), but shows elevated Al_2O_3 in the host rocks. A possible reason for this descrepancy with published data may be that the studied rocks are typically more evolved than melts in equilibrium with $Fo_{>84}$ and therefore likely have higher Al_2O_3 than melts, from which primitive assemblages of olivine and spinel were crystallized. In contrast, Kamenetsky et al. (2001) used compositions of melt inclusions in spinel to constrain this correlation, which are better representations of equilibrium melts. Additional evidence of compositional links between the host rocks and spinel is shown by correlating their TiO_2 contents (Fig. 5e). The apparent Ti partitioning is similar to that reported for other suites of magmatic spinel (Kamenetsky et al., 2001). The correlation of Al_2O_3 and TiO_2 in spinel and their host rocks shows that spinel crystallized from melts, which were compositionally similar to the bulk-rock composition. Therefore, the major and trace element compositions of the host rocks can be used to further evaluate major controls on spinel compositions (see sections 5.2, 5.3 and 5.4).

Kamenetsky et al. (2001) proposed using a TiO_2 vs. Al_2O_3 diagram for primitive spinel compositions in olivine Fo>84 to discriminate geodynamic settings. In this diagram, compositions of spinel from Kamchatka fall into the fields of arc basalts (CKD and EVF) and MORBs (SK, EVF, SR and NK) (Fig. 5f). In some samples, the MORB-like compositions of spinel can be explained by their back-arc origin (Kamenetsky et al., 2001). Spinel from SK and EVF represents frontal volcanoes in Kamchatka. Based on this data, the compositional field of island-arc spinel proposed by Kamenetsky et al. (2001) should be extended to include

part of the field of spinel from MORBs. The occurrence of low Cr# spinel in typical arc rocks, like those from the Kamchatka frontal volcanoes (SK, EVF), was also noted by Smith and Leeman (2005). A more robust criterion to distinguish spinel from arc and mid-ocean ridge settings is by comparing their different oxidation states. Low Cr# spinel from SK and EVF are significantly more oxidized in comparison with spinel from MORB, as we show in the following section.

5.2 Oxidation state of primitive Kamchatka magmas and its relation with host-rock compositions

The occurrence of Fe^{2+} and Fe^{3+} in Cr-spinel renders it one of the best indicators of redox conditions for the upper mantle spinel-lherzolites and basaltic magmas (Irvine, 1965), and has been applied in several models of spinel and olivine equilibria (Ballhaus et al., 1991; Mattioli and Wood, 1988; O'Neill and Wall, 1987). To estimate magma oxidation state from the composition of olivine and spinel in this study, we used a model proposed by Ballhaus et al. (1991). This model is sensitive to the presence of orthopyroxene in liquidus assemblage. However, recent studies have shown that this model and oxybarometer based on olivine-melt V partitioning (Shishkina et al., 2018; Nekrylov et al., 2018) yield similar estimates for ΔQFM within 0.5 units (ΔQFM is the deviation of fO_2 from that of quartz-fayalite-magnetite equilibria at given temperature expressed in log. units). Therefore, the model can be likely applied to primitive and moderately fractionated spinel compositions without correction for magma undersaturation in orthopyroxene. Temperature was calculated using Fe-Mg spinel-olivine equilibrium (Ballhaus et al., 1991). Pressure was assumed to be 0.1 GPa, which corresponds to the upper crustal conditions under Kamchatka. ΔQFM values estimated for different volcanic zones in Kamchatka are 1.7–2.1 (on average 1.9 ± 0.32, 2σ) for SK (except for basaltic cones at Opala caldera with ΔQFM ~ 1.3), 1.1–2.4 (on average 1.61 ± 0.76, 2σ)

for EVF, 1.0–3.7 (on average 1.72 ± 0.84, 2σ) for CKD, 1.2–1.7 (on average 1.45 ± 0.44, 2σ) for SR and 0.7–1.1 (on average 0.9 ± 0.44, 2σ) for NK.

Our data shows that primitive Kamchatka magmas are significantly more oxidized compared to MORBs, which typically crystallize at ΔQFM= +0.1 ± 0.2 (Cottrell and Kelley, 2011). Oxidizing conditions, which were estimated for Kamchatka, are typical for arc magmas (ΔQFM from +1 to +2, according to Richards (2015)) and usually attributed to the transfer of large amounts of ferric iron and other oxidized redox-sensitive elements into the mantle wedge from subducted hydrothermally altered oceanic crust (Evans, 2012; Kelley and Cottrell, 2009). The lowest ΔQFM in Kamchatka was estimated for SR and NK, where magmas originate from mantle sources with the smallest contribution of subduction-related components (Churikova et al., 2001; Volynets et al., 2010), or by pure pressure-release melting (Portnyagin et al., 2005a).

The dependence of ΔQFM in Kamchatka magmas on the extent of subduction-related metasomatism of their sources is supported by a statistically significant correlation between ΔQFM and indices of slab-derived components, such as La/Nb and Ba/La (e.g., Hanyu et al., 2006; Kelley and Cottrell, 2009), in bulk-rock composition. A particularly strong correlation is observed for samples from SR and NK. However, the correlation is not significant for EVF, CKD and SK. Nevertheless, the general regional trend of increasing ΔQFM with increasing subduction-related signature in Kamchatka rocks is still evident. This correlation suggests that the oxidation state of Kamchatka magmas and their sources is largely controlled by the amount of slab-derived components that interacted with the mantle wedge and caused coupled mantle oxidation and enrichment in fluid mobile elements. Similar correlations between Ba/La and melt oxidation state were reported for Mariana arc (Brounce et al., 2014) and for arc melts in general (Kelley and Cottrell, 2009).

Our data testifies that there is no significant difference in the estimated ΔQFM between different zones of the Eastern Kamchatka Volcanic Belt (Supplementary Table 4; Fig. 7a).

However, the ΔQFM estimates are highly variable for CKD volcanoes, especially for those from the northern CKD. These variations are also manifested in the composition of spinel inclusions in olivine Fo>88 (Supplementary Table 4), and therefore they cannot be explained by variable magma fractionation and oxidation. Since the minimum value of the estimated ΔQFM for CKD samples is nearly the same as for EVF and SK, these large variations can be caused by an additional oxidating agent involved in the magma generation beneath CKD, which could be represented by slab-derived melts (Portnyagin et al., 2007a; Yogodzinski et al., 2001), as discussed in section 5.4.

Some authors have proposed that the contribution of slab-derived components to arc mantle sources decreases from arc front to rear-arc (e.g., Ishikawa and Nakamura, 1994). However, we observed no significant correlations between ΔQFM and the depth from volcanoes to the Wadati-Benioff zone (Fig. 6c). This suggests that the amount of oxidizing slab-derived components may be relatively constant across the Kamchatka Arc, at least in parts, where the Wadati-Benioff zone is well defined. This does not negate the fact that composition of this component changes from relatively trace-element-poor fluid in the front of the volcanic arc to trace-element-rich hydrous silicate melt in the rear arc (e.g., Duggen et al., 2007; Portnyagin et al., 2007b).

It is noteworthy that primitive Kamchatka magmas with the highest Ba/La and La/Nb are not oxidized more than ΔQFM = 2 (Supplementary Table 4, Fig. 6). This indicates that their oxidation state may be buffered by some mineral equilibria in the sub-arc mantle under Kamchatka. A possible candidate for such buffering reaction is the equilibrium between sulfide and sulfate phases, which can coexist at ΔQFM = 0–2 at low pressures and at ΔQFM up to 3.5 at mantle wedge conditions for wide range of melt compositions (Jugo et al., 2010; Matjuschkin et al., 2016). This reaction can buffer the mantle wedge oxidation state either through oxidation of mantle sulfides by slab-derived fluids (e.g., Brounce et al., 2014), or

through reduction of trisulfur ion (S_3^-) (Pokrovski and Dubrovinsky, 2011) and/or SO_4^{2-} (Benard et al., 2018) from slab-derived fluids by sulfide precipitation (Rielli et al., 2017).

5.3. Constraints on mantle wedge depletion under Kamchatka from spinel composition

Spinel Cr# is commonly considered a useful indicator of the degree of mantle source depletion in basaltic systems (Arai, 1994; Dick and Bullen, 1984). The. Cr/Al ratio in mantle residues, primary melts and consequently in their equilibrium spinel increases with increasing degree of partial melting of spinel peridotite (e.g., Hellebrand et al., 2001; Jaques and Green, 1980). A direct application of the proposed equations linking Cr# in spinel and degree of mantle melting to volcanic rocks is complicated by significant dependence of the Al partitioning between spinel and melt on pressure (Barnes and Roeder, 2001; Sobolev and Danyushevsky, 1994). The liquidus spinel Cr# does not exactly correspond to spinel Cr# in the residual mantle, when significant difference exist between the pressures of melting and crystallization (Sobolev and Danyushevsky, 1994). In general, Cr# of spinel from volcanic rocks is informative about maximum degree of melting. This uncertainty decreases with decreasing differences between pressure of crystallization and pressure of the last melt equilibrium with mantle peridotite.

The Cr# of primitive spinel from SK, EVF and CKD closely corresponds to the Cr# of spinel from mantle xenoliths in some Kamchatka volcanic rocks and extends to lower values (Cr# < 40) (Fig. 5a). The mantle xenoliths were described in detail for the Avachinsky (Ionov, 2010), Bezymianny (Shcherbakov and Plechov, 2010) and Shiveluch (Bryant et al., 2007) volcanoes. The majority of them are represented by harzburgites with spinel Cr# = 40–80, which corresponds to the residual mantle formed by more than or equal to 15% of near fractional melting, or even in excess of 20% (Hellebrand et al., 2001; Jaques and Green, 1980). In comparison with spinel in mantle xenoliths, primitive spinel in Kamchatka volcanic rocks has a wider range of Cr# = 20–80, which corresponds to a range of degrees of melting

from ~8 to more than 20 %. The lowest degrees of melting (F < 15 %) and lherzolite residues (spinel Cr# < 0.4) are predicted for samples from SR, NK and some samples from EVF and SK. Harzburgite residues and F > 15% are typical in most parts of the Eastern Kamchatka Volcanic Belt (SK, EVF, CKD), and the most depleted residues are expected after extraction of CKD magmas (Fig. 5a, 7b).

Available data suggest that the parental magmas of Kamchatka volcanoes begin to crystallize in the lower crust at pressures of ~1 GPa (e.g., Gavrilenko et al., 2016; Kersting and Arculus, 1994; Portnyagin et al., 2005b). Assuming that the pressure of the last equilibria of the parental melts with mantle peridotite was 2 GPa, the difference in spinel Cr# between mantle residue and magmatic spinel should not exceed 10 mol.% (Sobolev and Danyushevsky, 1994). The degrees of melting for Kamchatka mantle source(s) calculated from the model of Hellebrand et al. (2001) can thus be overestimated by 2–3 %. This uncertainty is considered to be small and does not significantly exceed the uncertainty related to the spread of spinel Cr# for a single rock samples.

Our observations showing significantly higher degrees of partial melting under the Eastern Volcanic Belt compared to SR and NK are in general agreement with published data on the composition of mantle xenoliths in Kamchatka rocks and with independent geochemical modeling of bulk-rock and melt inclusion compositions (Churikova et al., 2001; Portnyagin et al., 2007b, 2015). The estimated degrees of mantle melting correlate with decreasing flux of hydrous fluids and melts into the mantle wedge, as the subducting slab under Kamchatka sinks into the mantle and dehydrates. The fluid-fluxed melting regime appears to be a predominant process under Kamchatka (Portnyagin et al., 2007b), with possible exceptions in the most northern volcanoes in SR and NK (Portnyagin et al., 2005).

5.4. Evidence for mantle re-fertilization by Ti-rich melts under CKD

Ti is moderately incompatible element during partial melting (Jaques and Green, 1980), and its concentration in primary magmas should provide information on the extent of this process (e.g., Stolper, Newman, 1994). Ti in primitive spinel correlates with melt composition (e.g., Kamenetsky et al., 2001), and therefore it can also be considered as a potential indicator of the mantle depletion and degree of partial melting.

In order to quantitatively estimate the degree of partial mantle melting from Ti content in liquidus spinel, the TiO_2 content in melt resulting from DMM melting and TiO_2 content in equilibrium spinel should be calculated. TiO_2 in model partial mantle melts was calculated using the TiO_2 content of the enriched DMM (0.132 wt.%), bulk partition coefficient (0.058) (Workman and Hart, 2005) and the equation of batch melting (Shaw, 1970):

$$TiO_2^{Melt} = \frac{0.132}{0.058 + F * 0.942} \quad \{1\}$$

Where F is a melt weight fraction.

Using data from Kamenetsky et al. (2001), the dependence of TiO_2 content in spinel on TiO_2 content in melt for island arc basalts can be expressed as follows:

$$TiO_2^{Sp} = 0.8 * (TiO_2^{Melt})^{1.2}. \quad \{2\}$$

By substituting TiO_2^{melt} with the equation of partial mantle melting and re-arranging the resulting equation, it is possible to calculate degree of DMM melting from the equilibrium concentration TiO_2 in spinel. The resulting equation is:

$$F = -0.06158 + 0.11635 * (TiO_2^{sp})^{-0.833}, \quad \{3\}$$

This equation can be used only for spinel in equilibrium with high-Fo olivine (Fo>88) because of the strong influence of magma fractionation on TiO_2 content in spinel. Spinel in equilibrium with high-Fo olivine in this study only occurs in the EVF and CKD. For the EVF spinel, we found a strong correlation between spinel Cr# and degrees of mantle melting of 16–22% calculated from TiO_2 in spinel using equation {3} (Fig. 8). In contrast, the data for CKD samples are very scattered and did not display any correlation between Cr# and TiO_2 in

spinel. A strong correlation for the EVF supports the view that spinel composition is informative on the degrees of mantle melting, however, data for the CKD seem to compromise it. The minor discrepancy between the trend of TiO_2-Cr#-based melting degrees for EVF and 1:1 line for these estimations can be explained by the pressure difference between mantle residue and magmatic spinel crystallization, which affects Cr#-based estimations (see section 5.3).

CKD magmas are clearly anomalous in the Kamchatka arc due to large variations in the estimated ΔQFM, highly variable spinel TiO_2 content and diverse bulk-rock geochemistry (Figs. 6, 7). A number of models have been proposed to explain this abundant and geochemically distinct volcanism in CKD: 1) unusually large flux of hydrous fluids/melts from the subducting Emperor Seamounts (e.g., Churikova et al., 2001; Dorendorf et al., 2000b); 2) slab melting at the Pacific slab edge under the northern CKD (Munker et al., 2004; Yogodzinski et al., 2001) or the entire group of CKD volcanoes (Portnyagin et al., 2007a); 3) interaction of the ascending melts with previously hydrothermally altered lithospheric mantle (Auer et al., 2009; Portnyagin et al., 2007a).

The presently available data does not permit us to fully reconcile the possible influence of these processes on the oxidation and enrichment of the mantle under CKD. It is, however, plausible that the contribution from Ti-rich slab- or mantle lithosphere-derived melts can cause re-fertilization of the mantle under CKD and decoupling between spinel TiO_2 and Cr#. If the model is correct, then care should be taken in estimating the degree of mantle melting of subduction-related magmas based on the widely accepted modeling of fluid-immobile elements in primitive rock and melt inclusion compositions (Stolper, Newman, 1994; Pearce and Parkinson, 1993; Portnyagin et al., 2007b). Alternative and potentially more accurate estimates can be obtained from spinel Cr#, which is not as easily modified as TiO_2 in depleted mantle.

6. Conclusions

We present a comprehensive compositional dataset of 1604 olivine-hosted Cr-spinel inclusions from 104 samples representing 30 volcanoes from all main late Quaternary volcanic zones in Kamchatka. This data places new constraints on regional variations of the magma oxidation state and the degrees of partial mantle melting under Kamchatka.

1) The oxidation state of parental magmas in Kamchatka varies from ΔQFM = +0.7 to +3.7. For Sredinny Range and Northern Kamchatka ΔQFM correlates with geochemical proxies of slab-derived components, such as Ba/La and La/Nb in the host-rocks, and suggests mantle oxidation by slab-derived fluid or melts.

2) The oxidation state of the parental magmas of the Eastern Kamchatka Volcanic Belt varies mostly within the range of ΔQFM= +1 to +2. The lack of correlation between the estimated redox conditions and bulk-rock geochemistry for active volcanic front in Kamchatka suggests that the mantle oxidation state may be buffered by coexisting sulfide and sulfate phases in the mantle.

3) Variations of primitive spinel Cr# suggest the degree of mantle melting ranges from 8 % to more than 20 % under Kamchatka. The least depleted residues were estimated for magmas from the Sredinny Range and Northern Kamchatka, which have the smallest contribution from the subducting slab. Magmas from the Eastern Volcanic Belt and the Central Kamchatka Depression originate by larger degrees of melting, based on high spinel Cr#. However, these magmas are enriched in Ti and can originate from mantle, which was refertilized by slab- or mantle lithosphere-derived Ti-rich melts.

The results of our study demonstrate that the composition of Cr-spinel in volcanic rocks in combination with bulk-rock compositions is a useful tool to map regional variations of the mantle source depletion, oxidation state, and involvement of various slab derived components in island-arc magmatism.

Acknowledgements. We are grateful to Daniil V. Popov (University of Geneva) for insightful discussions, Oleg V. Dirksen and Maria M. Pevzner for providing samples. This study was funded by the Russian Science Foundation grant #16-17-10145 to NN and VSK, German Ministry for Education and Research (BMBF) KOMEX and KALMAR to MP, DFG-RFBR grants # 00-0504000, 16-55-12040 and German Science Foundation grant #Wo362/51-1 to GW and TCH.

References

Arai, S., 1992. Chemistry of chromian spinel in volcanic rocks as a potential guide to magma chemistry. Mineralogical Magazine 56, 173–184.

Arai, S., 1994. Compositional variation of olivine-chromian spinel in Mg-rich magmas as a guide to their residual spinel peridotites. Journal of Volcanology and Geothermal Research 59, 279–293.

Auer, S.L., Bindeman, I., Wallace, P., Ponomareva, V.V., Portnyagin, M., 2009. The origin of hydrous, high-$\delta^{18}O$ voluminous volcanism: Diverse oxygen isotope values and high magmatic water contents within the volcanic record of Klyuchevskoy volcano, Kamchatka, Russia. Contributions to Mineralogy and Petrology 157, 209–230, doi:210.1007/s00410-00008-00330-00410.

Avdeiko, G.P., Savelyev, D.P., Palueva, A.A., Popruzhenko, S.V., 2007. Evolution of the Kurile-Kamchatkan volcanic arcs and dynamics of the Kamchatka-Aleutian junction, in: Eichelberger, J., Gordeev, E., Izbekov, P., Kasahara, M., Lees, J. (Eds.), Volcanism and Subduction: The Kamchatka Region. American Geophysical Union, pp. 37–55.

Ballhaus, C., Berry, R.F., Green, D.H., 1991. High pressure experimental calibration of the olivine-orthopyroxene-spinel oxygen geobarometer: implications for the oxidation state of the upper mantle. Contributions to Mineralogy and Petrology 107, 27–40.

Barnes, S.J., Roeder, P.L., 2001. The range of spinel compositions in terrestrial mafic and ultramafic rocks. Journal of Petrology 42, 2279–2302.

Bénard, A., Klimm, K., Woodland, A.B., Arculus, R.J., Wilke, M., Botcharnikov, R.E., Shimizu, N., Nebel, O., Rivard, C., Ionov, D.A., 2018. Oxidising agents in sub-arc mantle melts link slab devolatilisation and arc magmas. Nature communications 9(1), 3500.

Bergal-Kuvikas, O., Nakagawa, M., Kuritani, T., Muravyev, Y., Malik, N., Klimenko, E., Amma-Miyasaka, M., Matsumoto, A., Shimada, S., 2017. A petrological and geochemical study on time-series samples from Klyuchevskoy volcano, Kamchatka arc. Contributions to Mineralogy and Petrology 172, 35.

Bindeman, I.N., Eiler, J.M., Yogodzinski, G.M., Tatsumi, Y., Stern, C.R., Grove, T.L., Portnyagin, M., Hoernle, K., Danyushevsky, L.V., 2005. Oxygen isotope evidence for slab melting in modern and ancient subduction zones. Earth and Planetary Science Letters 235, 480–496.

Brounce, M.N., Kelley, K.A., Cottrell, E., 2014. Variations in $Fe^{3+}/\Sigma Fe$ of Mariana arc basalts and mantle wedge fO_2. Journal of Petrology 55, 2514-2536.

Bryant, J.A., Yogodzinski, G.M., Churikova, T.G., 2007. Melt-mantle interactions beneath the Kamchatka arc: Evidence from ultramafic xenoliths from Shiveluch volcano. Geochemistry, Geophysics, Geosystems 8.

Churikova, T., Dorendorf, F., Wörner, G., 2001. Sources and fluids in the mantle wedge below Kamchatka, evidence from across-arc geochemical variation. Journal of Petrology 42, 1567–1593.

Churikova, T., Wörner, G., Mironov, N., Kronz, A., 2007. Volatile (S, Cl and F) and fluid mobile trace element compositions in melt inclusions: Implications for variable fluid sources across the Kamchatka arc. Contributions to Mineralogy and Petrology 154, 217–239.

Churikova, T.G., Gordeychik, B.N., Ivanov, B.V., Wörner, G., 2013. Relationship between Kamen Volcano and the Klyuchevskaya group of volcanoes (Kamchatka). Journal of Volcanology and Geothermal Research 263, 3–21.

Cottrell, E., Kelley, K.A., 2011. The oxidation state of Fe in MORB glasses and the oxygen fugacity of the upper mantle. Earth and Planetary Science Letters 305, 270–282.

Deering, C.D., Gravley, D.M., Vogel, T.A., Cole, J.W., Leonard, G.S., 2010. Origins of cold-wet-oxidizing to hot-dry-reducing rhyolite magma cycles and distribution in the Taupo Volcanic Zone, New Zealand. Contributions to Mineralogy and Petrology 160, 609–629.

DeMets, C., Gordon, R.G., Argus, D.F., Stein, S., 1990. Current plate motions. Geophysical Journal International 101, 425–478.

Dick, H.J.B., Bullen, T., 1984. Chromian spinel as a petrogenetic indicator in abyssal and alpine-type peridotites and spatially associated lavas. Contributions to Mineralogy and Petrology 86, 54–76.

Dirksen, O.V., Melekestsev, I.V., 1999. Chronology, dinamics of formation and eruptive centers morphology of Holocene stage of Avacha river basin areal volcanism (Kamchatka, Russia). Volcanology and Seismology 1, 3–19 (in russian).

Dorendorf, F., Churikova, T., Koloskov, A., Wörner, G., 2000a. Late Pleistocene to Holocene activity at Bakening volcano and surrounding monogenetic centers (Kamchatka): volcanic geology and geochemical evolution. Journal of Volcanology and Geothermal Research 104, 131–151.

Dorendorf, F., Wiechert, U., Worner, G., 2000b. Hydrated sub-arc mantle: a source for the Kluchevskoy volcano, Kamchatka/Russia. Earth & Planetary Science Letters 175, 69–86.

Duggen, S., Portnyagin, M., Baker, J., Ulfbeck, D., Hoernle, K., Garbe-Schönberg, D., Grassineau, N., 2007. Drastic shift in lava geochemistry in the volcanic-front to rear-arc region of the Southern Kamchatkan subduction zone: Evidence for the transition from slab surface dehydration to sediment melting. Geochimica et Cosmochimica Acta 71, 452–480.

Evans, K.A., 2012. The redox budget of subduction zones. Earth-Science Reviews 113, 11–32.

Ewart, A., Collerson, K.D., Regelous, M., Wendt, J.I., Niu, Y., 1998. Geochemical evolution within the Tonga-Kermadec-Lau arc-back-arc systems: the role of varying mantle wedge composition in space and time. Journal of Petrology 39, 331–368.

Gavrilenko, M., Ozerov, A., Kyle, P.R., Carr, M.J., Nikulin, A., Vidito, C., Danyushevsky, L., 2016. Abrupt transition from fractional crystallization to magma mixing at Gorely volcano (Kamchatka) after caldera collapse. Bulletin of Volcanology 78, 47.

Gorbach, N., Portnyagin, M., Tembrel, I., 2013. Volcanic structure and composition of Old Shiveluch volcano, Kamchatka. Journal of Volcanology and Geothermal Research 263, 193–208.

Gorbach, N.V., Portnyagin, M.V., 2011. Geology and petrology of the lava complex of Young Shiveluch Volcano, Kamchatka. Petrology 19, 134.

Gorbatov, A., Kostoglodov, V., Suárez, G., Gordeev, E., 1997. Seismicity and structure of the Kamchatka subduction zone. Journal of Geophysical Research B: Solid Earth 102, 17883–17898.

Gordeychik, B., Churikova, T., Kronz, A., Sundermeyer, C., Simakin, A., Wörner, G., 2018. Growth of, and diffusion in, olivine in ultra-fast ascending basalt magmas from Shiveluch volcano. Scientific Reports 8, 11775, doi: 10.1038/s41598-018-30133-1

Grib, E.N., Perepelov, A.B., 2008. Olivine basalts at the Karymskii Volcanic Center: Mineralogy, petrogenesis, and magma sources. Journal of Volcanology and Seismology 2, 228–247.

Hanyu, T., Tatsumi, Y., Nakai, S.I., Chang, Q., Miyazaki, T., Sato, K., Tani, K., Shibata, T., Yoshida, T., 2006. Contribution of slab melting and slab dehydration to magmatism in the NE Japan arc for the last 25 Myr: Constraints from geochemistry. Geochemistry, Geophysics, Geosystems, 7(8).

Hellebrand, E., Snow, J.E., Dick, H.J.B., Hofmann, A.W., 2001. Coupled major and trace elements as indicators of the extent of melting in mid-ocean-ridge peridotites. Nature 410, 677–681.

Hirth, G., Kohlstedt, D., 2003. Rheology of the Upper Mantle and the Mantle Wedge: A View from the Experimentalists, Inside the Subduction Factory, pp. 83–105.

Ionov, D.A., 2010. Petrology of Mantle Wedge Lithosphere: New Data on Supra-Subduction Zone Peridotite Xenoliths from the Andesitic Avacha Volcano, Kamchatka. Journal of Petrology 51, 327–361.

Irvine, T.N., 1965. Chromian spinel as a petrogenetic indicator. Part I. Theory. Canadian Journal of Earth Sciences 2, 648–671.

Ishikawa, T., Nakamura, E., 1994. Origin of the slab component in arc lavas from across-arc variation of B and Pb isotopes. Nature 370, 205.

Jaques, A.L., Green, D.H., 1980. Anhydrous melting of peridotite at 0–15 kb pressure and the genesis of tholeiitic basalts. Contributions to Mineralogy and Petrology 73, 287–310.

Jarosewich, E.J., Nelen, J.A., Norberg, J.A., 1980. Reference samples for electron microprobe analysis. Geostandards Newsletter 4, 43–47.

Jugo, P.J., Wilke, M., Botcharnikov, R.E., 2010. Sulfur K-edge XANES analysis of natural and synthetic basaltic glasses: Implications for S speciation and S content as function of oxygen fugacity. Geochimica et Cosmochimica Acta 74, 5926-5938.

Kamenetsky, V.S., Crawford, A.J., Meffre, S., 2001. Factors controlling chemistry of magmatic spinel: an empirical study of associated olivine, Cr-spinel and melt inclusions from primitive rocks. Journal of Petrology 42, 655–671.

Kelley, K.A., Cottrell, E., 2009. Water and the oxidation state of subduction zone magmas. Science 325, 605–607.

Kersting, A.B., Arculus, R.J., 1994. Klyuchevskoy volcano, Kamchatka, Russia: the role of high-flux recharged, tapped, and fractionated magma chamber(s) in the genesis of high-Al_2O_3 from high-MgO basalt. Journal of Petrology 35, 1–41.

Lander, A.V., Shapiro, M.N., 2007. The origin of the modern Kamchatka subduction zone, in: Eichelberger, J., Gordeev, E., Izbekov, P., Kasahara, M., Lees, J. (Eds.), Volcanism and Subduction: The Kamchatka Region. American Geophysical Union, pp. 57–64.

Leuthold, J., Blundy, J.D., Brooker, R.A., 2015. Experimental petrology constraints on the recycling of mafic cumulate: a focus on Cr-spinel from the Rum Eastern Layered Intrusion, Scotland. Contributions to Mineralogy and Petrology 170: 12.

Levin, V., Shapiro, N., Park, J., Ritzwoller, M., 2002. Seismic evidence for catastrophic slab loss beneath Kamchatka. Nature 418, 763.

Matjuschkin, V., Blundy, J.D., Brooker, R.A., 2016. The effect of pressure on sulphur speciation in mid-to deep-crustal arc magmas and implications for the formation of porphyry copper deposits. Contributions to Mineralogy and Petrology 171.

Mattioli, G.S., Wood, B.J., 1988. Magnetite activities across the $MgAl_2O_4$-Fe_3O_4 spinel join, with application to thermobarometric estimates of upper mantle oxygen fugacity. Contributions to Mineralogy and Petrology 98, 148–162.

Mironov, N., Portnyagin, M., Botcharnikov, R., Gurenko, A., Hoernle, K., Holtz, F., 2015. Quantification of the CO_2 budget and H_2O–CO_2 systematics in subduction-zone magmas through the experimental hydration of melt inclusions in olivine at high H_2O pressure. Earth and Planetary Science Letters 425, 1–11.

Münker, C., Wörner, G., Yogodzinski, G., Churikova, T., 2004. Behaviour of high field strength elements in subduction zones: constraints from Kamchatka-Aleutian arc lavas. Earth and Planetary Science Letters 224, 275–293.

Nazarova, D.P., Portnyagin, M.V., Krasheninnikov, S.P., Mironov, N.L., Sobolev, A.V., 2017. Initial H_2O content and conditions of parent magma origin for Gorely volcano (Southern Kamchatka) estimated by trace element thermobarometry. Doklady Earth Sciences 472, 100–103.

Nekrylov, N., Popov, D., Plechov, P., Shcherbakov, V., Danyushevsky, L., Dirksen, O.V., 2018. Garnet-pyroxenite-derived end-member magma type in Kamchatka: evidence from composition of olivine and olivine-hosted melt inclusions in Holocene rocks of Kekuknaisky volcano. Petrology 26, 329–350.

O'Neill, H.S.C., Wall, V.J., 1987. The olivine-orthopyroxene-spinel oxygen geobarometer, the nickel precipitation curve, and the oxygen fugacity of the Earth's upper mantle. Journal of Petrology 28, 1169–1191.

Park, J., Levin, V., Brandon, M., Lees, J., Peyton, V., Gordeev, E., Ozerov, A., 2002. A Dangling Slab, Amplified Arc Volcanism, Mantle Flow and Seismic Anisotropy in the Kamchatka Plate Corner, Plate Boundary Zones. American Geophysical Union, pp. 295–324.

Pearce, J.A., Parkinson, I.J., 1993. Trace element models for mantle melting: application to volcanic arc petrogenesis. Geological Society, London, Special Publications 76, 373.

Peate, D.W., Pearce, J.A., Hawkesworth, C.J., Colley, H., Edwards, C.M.H., Hirose, K., 1997. Geochemical variations in Vanuatu arc lavas: the role of subducted material and a variable mantle wedge composition. Journal of Petrology 38, 1331–1358.

Plechova, A.A., Portnyagin, M.V., Bazanova, L.I., 2011. The origin and evolution of the parental magmas of frontal volcanoes in Kamchatka: Evidence from magmatic inclusions in olivine from Zhupanovsky volcano. Geochemistry International 49, 743.

Pokrovski, G.S., Dubrovinsky, L.S., 2011. The S_3^- ion is stable in geological fluids at elevated temperatures and pressures. Science 331, 1052–1054.

Ponomareva, V.V., Melekestsev, I.V., Braitseva, O.A., Churikova, T., Pevzner, M.M., Sulerzhitsky, L.D., 2007. Late Pleistocene- Holocene Volcanism on the Kamchatka Peninsula, Northwest Pacific Region, Volcanism and Subduction: The Kamchatka Region, pp. 165–198.

Portnyagin, M., Bindeman, I., Hoernle, K., Hauff, F., 2007a. Geochemistry of primitive lavas of the Central Kamchatka Depression: magma generation at the edge of the Pacific Plate, in: Eichelberger, J., Gordeev, E., Izbekov, P., Kasahara, M., Lees, J. (Eds.), Volcanism and subduction: the Kamchatka region, pp. 199–239.

Portnyagin, M., Duggen, S., Hauff, F., Mironov, N., Bindeman, I., Thirlwall, M., Hoernle, K., 2015. Geochemistry of the late Holocene rocks from the Tolbachik volcanic field, Kamchatka: Quantitative modelling of subduction-related open magmatic systems. Journal of Volcanology and Geothermal Research 307, 133–155.

Portnyagin, M., Hoernle, K., Avdeiko, G., Hauff, F., Werner, R., Bindeman, I., Uspensky, V., Garbe-Schönberg, D., 2005a. Transition from arc to oceanic magmatism at the Kamchatka-Aleutian junction. Geology 33, 25–28.

Portnyagin, M., Hoernle, K., Plechov, P., Mironov, N., Khubunaya, S., 2007b. Constraints on mantle melting and composition and nature of slab components in volcanic arcs from volatiles (H_2O, S, Cl, F) and trace elements in melt inclusions from the Kamchatka Arc. Earth and Planetary Science Letters 255, 53–69.

Portnyagin, M.V., Plechov, P.Y., Matveev, S.V., Osipenko, A.B., Mironov, N.L., 2005b. Petrology of avachites, high-magnesian basalts of Avachinsky volcano, Kamchatka: I. General characteristics and composition of rocks and minerals. Petrology 13, 99–121.

Prouteau, G., Scaillet, B., Pichavant, M., Maury, R., 2001. Evidence for mantle metasomatism by hydrous silicic melts derived from subducted oceanic crust. Nature 410, 197.

Richards, J.P., 2015. The oxidation state, and sulfur and Cu contents of arc magmas: implications for metallogeny. Lithos 233, 27–45.

Rielli, A., Tomkins, A.G., Nebel, O., Brugger, J., Etschmann, B., Zhong, R., Yaxley, G.M., Paterson, D., 2017. Evidence of sub-arc mantle oxidation by sulphur and carbon. Geochemical Perspectives Letters 6, 124–132.

Shaw, D.M., 1970. Trace element fractionation during anatexis. Geochimica et Cosmochimica Acta, 34(2), 237–243.

Shcherbakov, V.D., Plechov, P.Y., 2010. Petrology of mantle xenoliths in rocks of the Bezymyannyi Volcano (Kamchatka). Doklady Earth Sciences 434, 1317–1320.

Shishkina, T.A., Portnyagin, M., Botcharnikov, R., Almeev, R.R., Simonyan, D., Garbe-Schonberg, D., Schuth, S., Oeser, M., Holtz, F., 2018. Experimental calibration and implications of olivine-melt vanadium oxybarometry for hydrous basaltic arc magmas. American Mineralogist 103, 369–383.

Smith, D.R., Leeman, W.P., 2005. Chromian spinel-olivine phase chemistry and the origin of primitive basalts of the southern Washington Cascades. Journal of Volcanology and Geothermal Research 140, 49–66.

Sobolev, A.V., Danyushevsky, L.V., 1994. Petrology and geochemistry of boninites from the north termination of the Tonga Trench: constraints on the generation conditions of primary high-Ca boninite magmas. Journal of Petrology 35, 1183–1211.

Stolper, E., Newman, S., 1994. The role of water in the petrogenesis of Mariana trough magmas. Earth and Planetary Science Letters, 121(3–4), 293–325.

Su, B.X., Teng, F.Z., Hu, Y., Shi, R.D., Zhou, M.F., Zhu, B., Liu, F., Gong X.-H., Huang Q.-S., Xiao Y., Chen C., He Y.-S., 2015. Iron and magnesium isotope fractionation in oceanic lithosphere and sub-arc mantle: Perspectives from ophiolites. Earth and Planetary Science Letters 430, 523–532.

Tatsumi, Y., Eggins, S., 1995. Subduction zone magmatism. Blackwell Science, Inc. P.211

Tobelko, D.P., Portnyagin, M., Krasheninnikov, S.P., Grib, E.N., Plechov, P., 2019. Initial H_2O content and conditions of parent magma origin for Karymsky volcano estimated by melt inclusions study and trace element thermobarometry. Russian Geology and Geophysics In press.

Ulmer, P., 2001. Partial melting in the mantle wedge — the role of H_2O in the genesis of mantle-derived 'arc-related' magmas. Physics of the Earth and Planetary Interiors 127, 215–232.

Volynets, A.O., Churikova, T.G., Worner, G., Gordeychik, B.N., Layer, P., 2010. Mafic Late Miocene-Quaternary volcanic rocks in the Kamchatka back arc region: implications for

subduction geometry and slab history at the Pacific-Aleutian junction. Contributions to Mineralogy and Petrology 159, 659–687.

Volynets, O.N., 1994. Geochemical Types, Petrology, and Genesis of Late Cenozoic Volcanic Rocks from the Kurile-Kamchatka Island-Arc System. International Geology Review 36, 373–405.

Volynets, O.N., Babanskii, A.D., Gol'tsman, Y.V., 2000. Variations in isotopic and trace-element composition of lavas from volcanoes of the Northern group, Kamchatka, in relation to specific features of subduction. Geochemistry International 38, 974–989.

Wan, Z.H., Coogan, L.A., Canil, D., 2008. Experimental calibration of aluminum partitioning between olivine and spinel as a geothermometer. American Mineralogist 93, 1142-1147.

Workman, R.K., Hart, S.R., 2005. Major and trace element composition of the depleted MORB mantle (DMM). Earth and Planetary Science Letters 231, 53–72.

Yogodzinski, G.M., Lees, J.M., Churikova, T.G., Dorendorf, F., Wöerner, G., Volynets, O.N., 2001. Geochemical evidence for the melting of subducting oceanic lithosphere at plate edges. Nature 409, 500.

Zhao, D., Pirajno, F., Dobretsov, N.L., Liu, L., 2010. Mantle structure and dynamics under East Russia and adjacent regions. Russian Geology and Geophysics 51, 925–938.

Figure captions

Fig. 1. Map of late Quaternary volcanism in Kamchatka. The distribution of late Quaternary volcanics is shown by grey fields (Ponomareva et al., 2007). Dashed lines mark the depth of the Wadati-Benioff zone (Gorbatov et al., 1997). Numbers indicate volcanoes and volcanic fields in the areas of South Kamchatka (1–9), Eastern Volcanic Front (10–16), Central Kamchatka Depression (17–24), Sredinny Range (26–29) and Northern Kamchatka (30) which were studied in our work: 1 – Bol'shaya Ipel'ka; 2 – Savan River; 3 – Asacha; 4 – Opala; 5 – Tolmachev Dol volcanic field; 6 – Tolmachev; 7 – Mutnovsky; 8 – Gorely; 9 – Barkhatnaya Sopka; 10 – Avachinsky; 11 – Zhupanovsky; 12 – Bakening; 13 – Karymsky; 14 – Schmidt; 15 – Gamchen; 16 – Komarov; 17 – Tolbachik; 18 – Kamen; 19 – Klyuchevskaya Sopka; 20 – Ploskie Sopki volcanic massif; 21 – Harchinsky; 22 – Zarechny; 23 – Shiveluch; 24 – Shisheisky complex; 25 – Ichinsky; 26 – Akhtang; 27 – Kekuknaisky volcanic field; 28 – Sedanka volcanic field; 29 – Tobeltsen; 30 – Nachikinsky.

Fig. 2. Bulk-rock composition of studied samples from different volcanic zones of Kamchatka. Data sources are listed in Supplementary Table 1. .Volcanic rocks of Kamchatka are shown for comparison (GEOROC database).

Fig. 3. Histograms of host-olivine Fo-number for different volcanic zones of Kamchatka. N is the number of analyses.

Fig. 4. Composition of Cr-spinel inclusions in olivine from volcanic rocks of Kamchatka. (a) Ternary Al-Cr-Fe^{3+} diagram, (b) spinel Mg# vs. olivine Fo, (c) spinel Cr# vs. olivine Fo, (d) spinel Cr# vs. spinel Mg# averaged by sample for inclusions in olivine Fo_{84-86} (Supplementary Table 3), (e) spinel Fe^{2+}/Fe^{3+} vs. olivine Fo.

Fig. 5. Average compositions of Cr-spinel inclusions in olivine $Fo_{>84}$ (Supplementary Table 4) from studied samples. Large symbols denote average compositions of coexisting Fo-rich olivine and spinel in one rock sample. (a) Spinel Cr# vs. host-olivine Fo. Grey field indicates Olivine-Spinel Mantle Array (OSMA) after (Arai, 1994). Dashed lines delineate compositions of coexisting olivine and spinel from mantle xenoliths in Kamchatka volcanic rocks (Bryant et al., 2007, Ionov, 2010, Shcherbakov & Plechov, 2010); (b) Spinel Mg# vs. host-olivine Fo. (c) Spinel Fe^{2+}/Fe^{3+} vs. host-olivine Fo; (d) spinel Al_2O_3 vs. bulk-rock Al_2O_3 content. Grey dashed curve shows equilibrium compositions after Kamenetsky et al. (2001). (e) Spinel TiO_2 vs. bulk-rock TiO_2. The dashed and solid grey lines indicate best fit for spinels with Al_2O_3 < 15 wt.% and > 19 wt.%, respectively (Kamenetsky et al., 2001); (f) Spinel TiO_2 vs. spinel Al_2O_3 diagram. Fields of typical spinel composition for arcs, MORBs, LIPs and OIBs are after Kamenetsky et al. (2001). Small grey symbols on figures (a) and (b) show compositions of the most evolved spinel for CKD samples and for 2 samples containing Cr-rich spinel from EVF.

Fig. 6. Redox conditions of magma crystallization estimated from composition of coexisting spinel and olivine ($Fo_{>84}$ – open symbols; $Fo_{>88}$ – filled symbols (Supplementary Table 4)) in Kamchatka rocks vs. bulk-rock compositions (a, b) and depth from volcano to the Wadati-Benioff zone (c) (Gorbatov et al., 1997). Diagrams (a) and (b) are drawn using ICP-MS trace element data for bulk-rocks; low precision XRF data is not shown. Diagram (c) shows data only for those volcanoes where the Wadati-Benioff zone is detected. Vertical dashed lines define ΔQFM = +2 – maximal oxidation level for Kamchatka magmas. The grey field delineates the data from the Mariana Arc (Brounce et al., 2014).

Fig. 7. South to north spatial variability of the estimated redox conditions (a), Cr# (b) and TiO_2 content (c) for spinel hosted in olivine $Fo_{>84}$ (clear symbols) and in olivine $Fo_{>88}$

(filled symbols) (Supplementary Table 4). In plot (b) degrees of mantle melting are shown as a function of spinel Cr# after Hellebrandt et al. (2000)

Fig. 8. Degree of melting estimated from TiO_2 content in spinel inclusions in high-Fo olivine ($Fo_{>88}$) vs. their Cr#. The black line marks the 1:1 line for the melting degree estimated from spinel TiO_2 content and from spinel Cr# following the model of Hellebrand et al (2001). The values of Cr#-based melting degree, corresponding to Cr# > 60, are the extrapolation and marked by the dashed line.

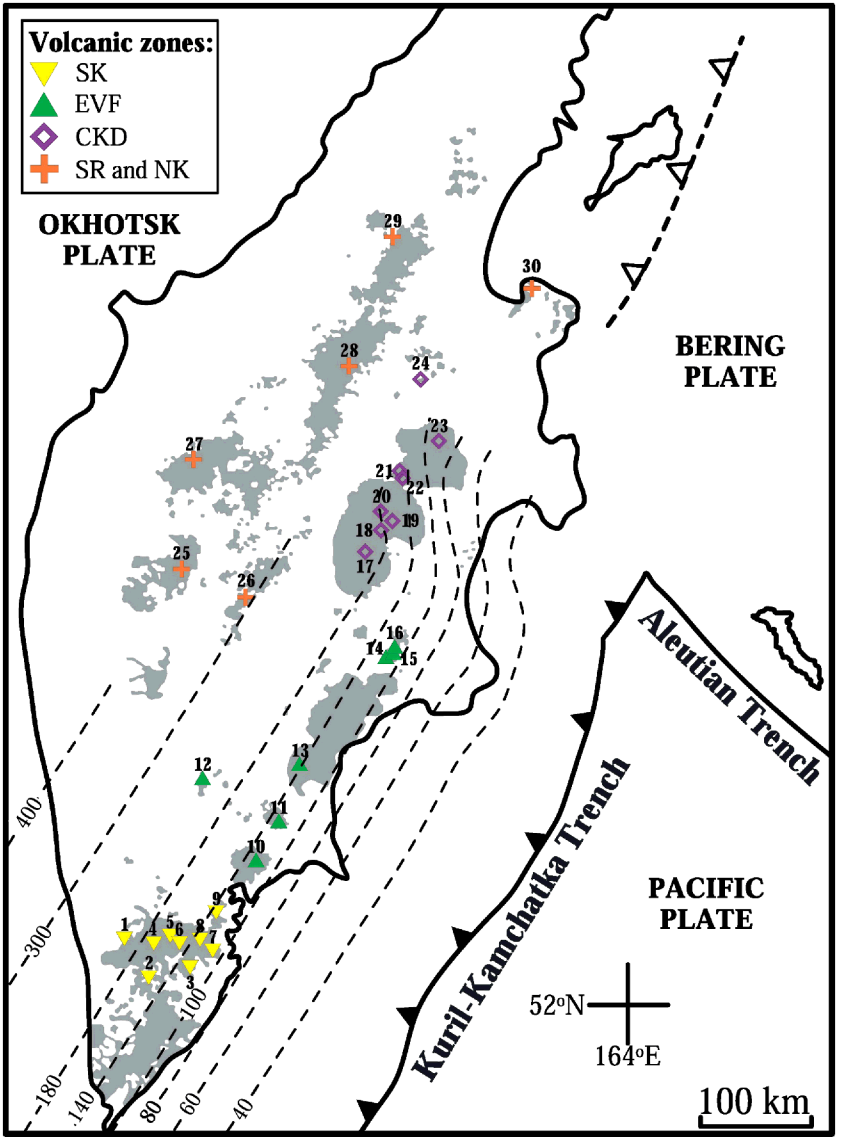
Volcanic zones:
SK
EVF
CKD
SR and NK
OKHOTSK PLATE
BERING PLATE
PACIFIC PLATE
Aleutian Trench
Kuril-Kamchatka Trench
52°N
164°E
100 km
400
300
180
140
100
80
60
40
1
2
3
4
5
6
7
8
9
10
11
12
13
14
15
16
17
18
19
20
21
22
23
24
25
26
27
28
29
30

Figure 1

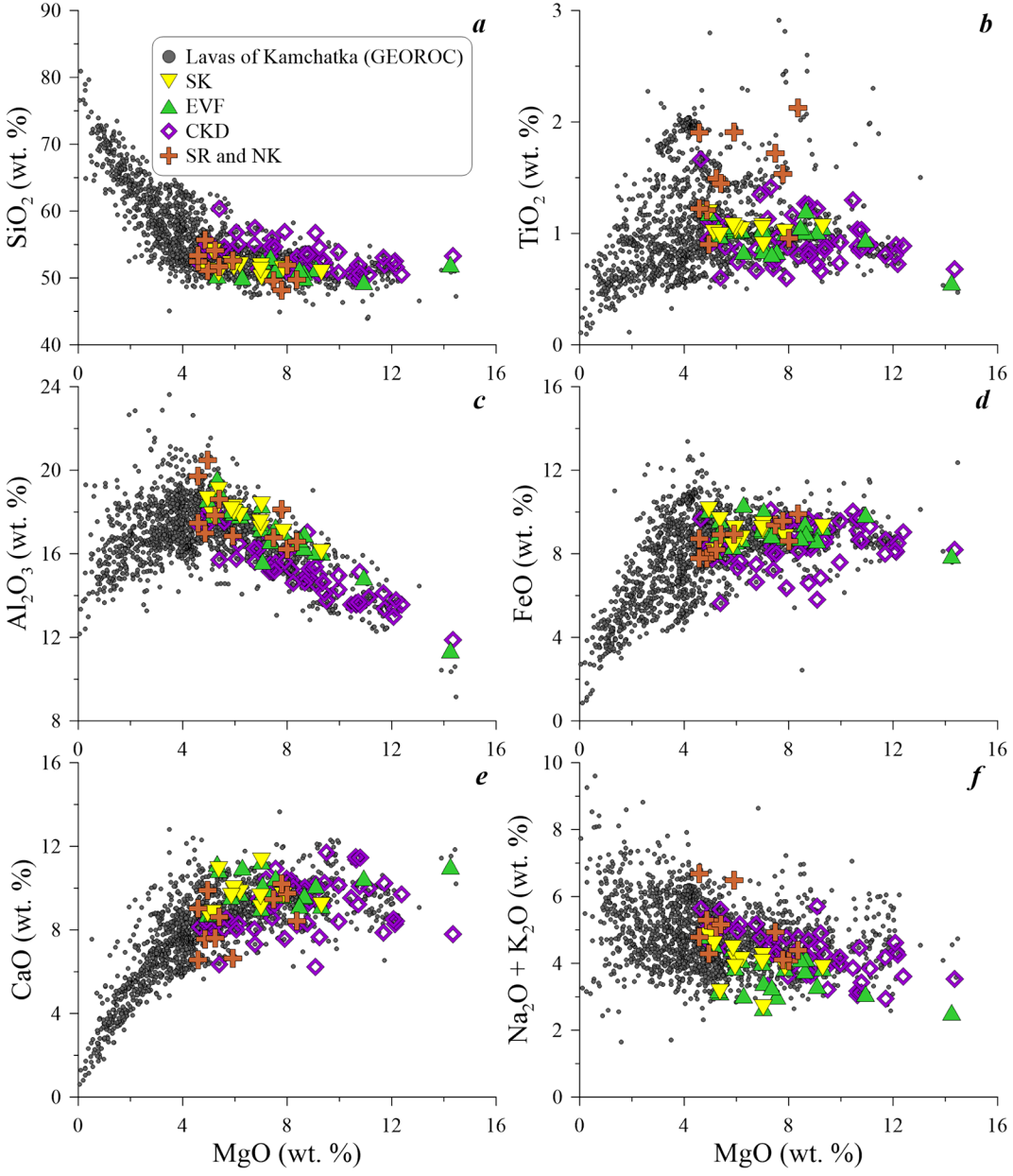
a
b
c
d
e
f
Lavas of Kamchatka (GEOROC)
SK
EVF
CKD
SR and NK
SiO2 (wt. %)
TiO2 (wt. %)
Al2O3 (wt. %)
FeO (wt. %)
CaO (wt. %)
Na2O + K2O (wt. %)
MgO (wt. %)
MgO (wt. %)

Figure 2

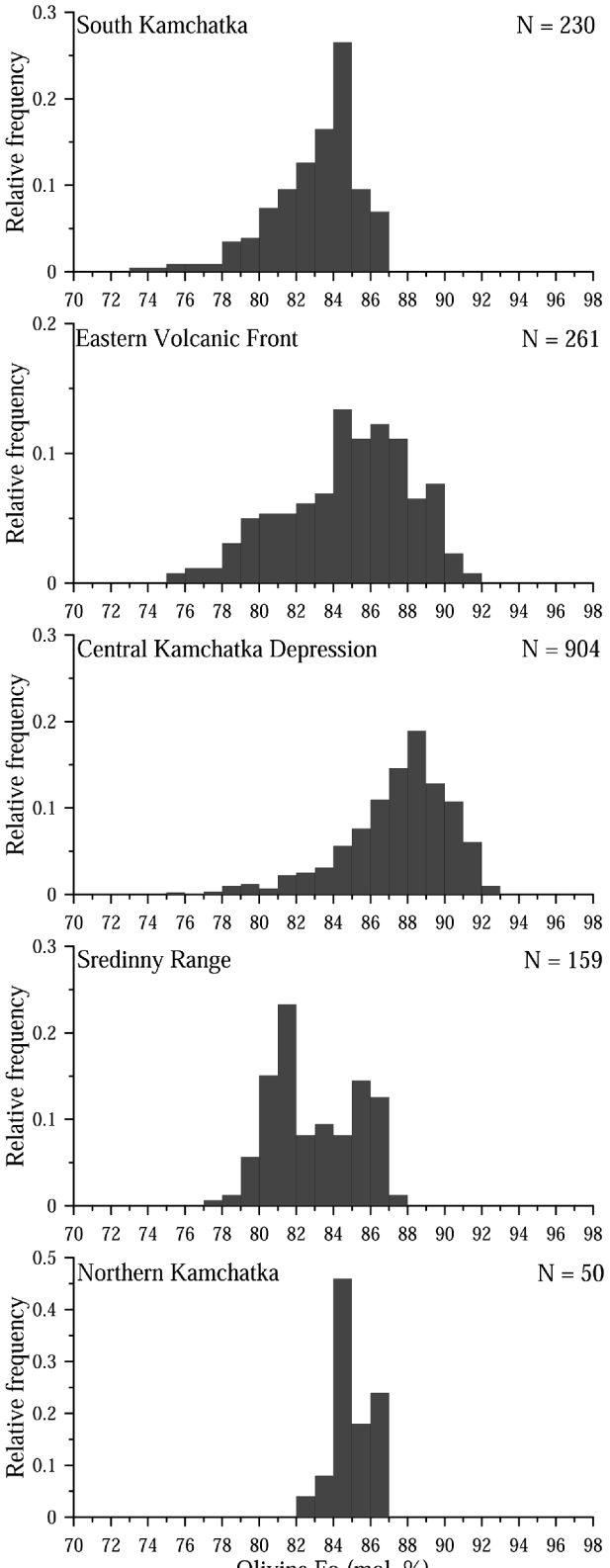
South Kamchatka
N = 230
Eastern Volcanic Front
N = 261
Central Kamchatka Depression
N = 904
Sredinny Range
N = 159
Northern Kamchatka
N = 50
Relative frequency
Olivine Fo (mol. %)

Figure 3

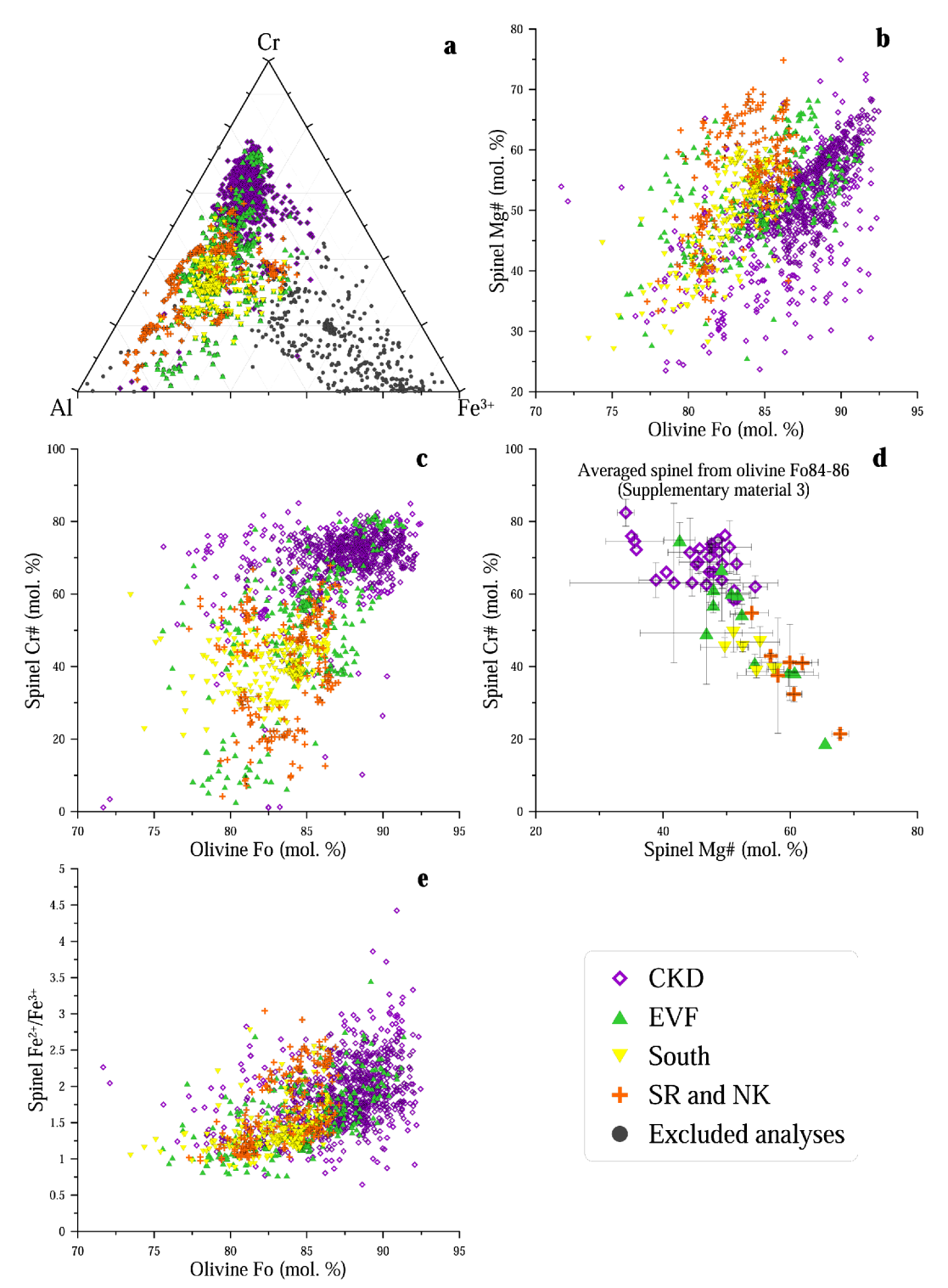
a
Cr
Al
Fe3+
b
Spinel Mg# (mol. %)
Olivine Fo (mol. %)
c
Spinel Cr# (mol. %)
Olivine Fo (mol. %)
d
Averaged spinel from olivine Fo84-86
(Supplementary material 3)
Spinel Cr# (mol. %)
Spinel Mg# (mol. %)
e
Spinel Fe2+/Fe3+
Olivine Fo (mol. %)
CKD
EVF
South
SR and NK
Excluded analyses

Figure 4

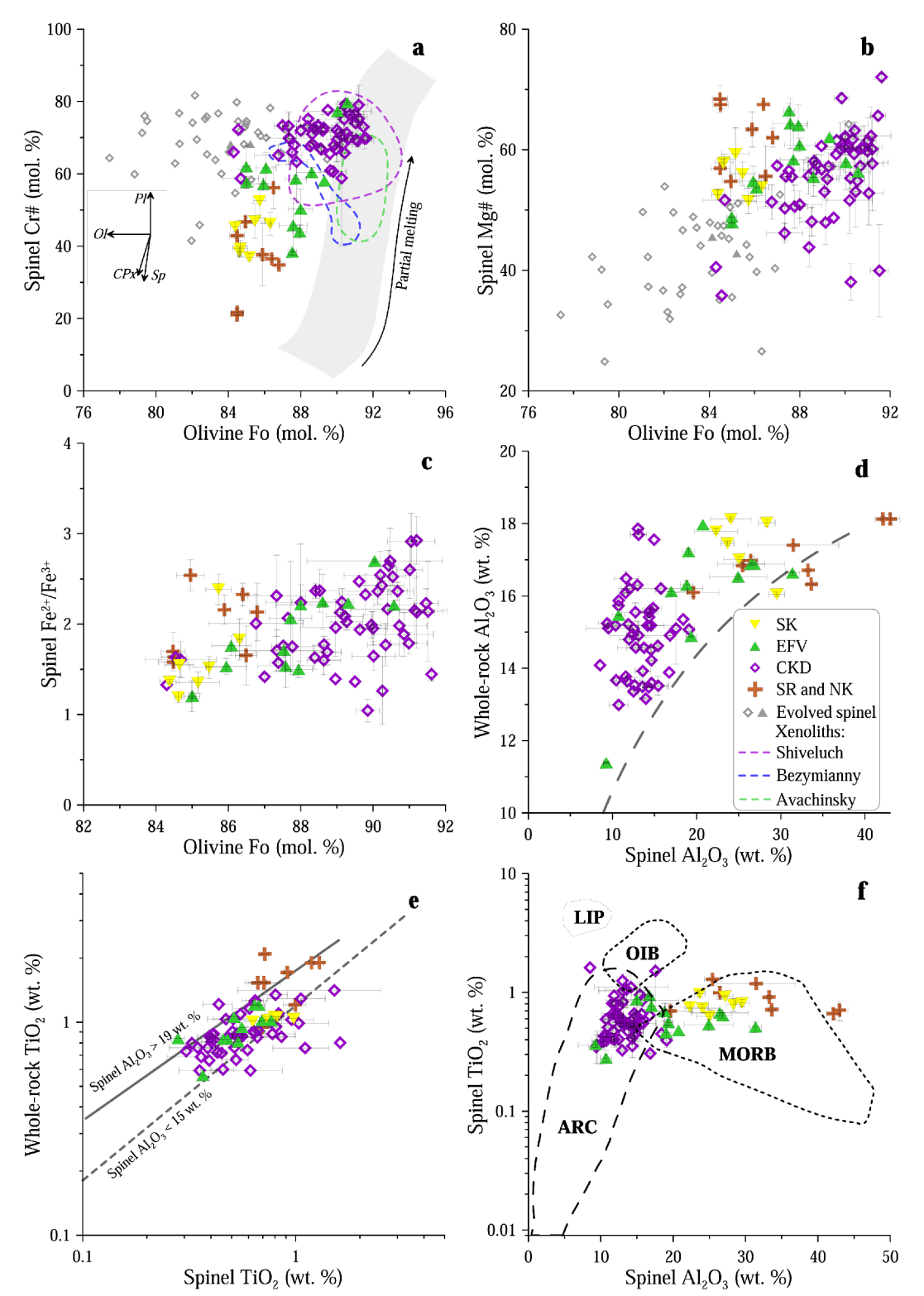
a
Spinel Cr# (mol. %)
Olivine Fo (mol. %)
Pl
Ol
CPx
Sp
Partial melting
b
Spinel Mg# (mol. %)
Olivine Fo (mol. %)
c
Spinel Fe2+/Fe3+
Olivine Fo (mol. %)
d
Whole-rock Al2O3 (wt. %)
Spinel Al2O3 (wt. %)
SK
EFV
CKD
SR and NK
Evolved spinel
Xenoliths:
Shiveluch
Bezymianny
Avachinsky
e
Whole-rock TiO2 (wt. %)
Spinel TiO2 (wt. %)
Spinel Al2O3 > 19 wt. %
Spinel Al2O3 < 15 wt. %
f
Spinel TiO2 (wt. %)
Spinel Al2O3 (wt. %)
LIP
OIB
MORB
ARC

Figure 5

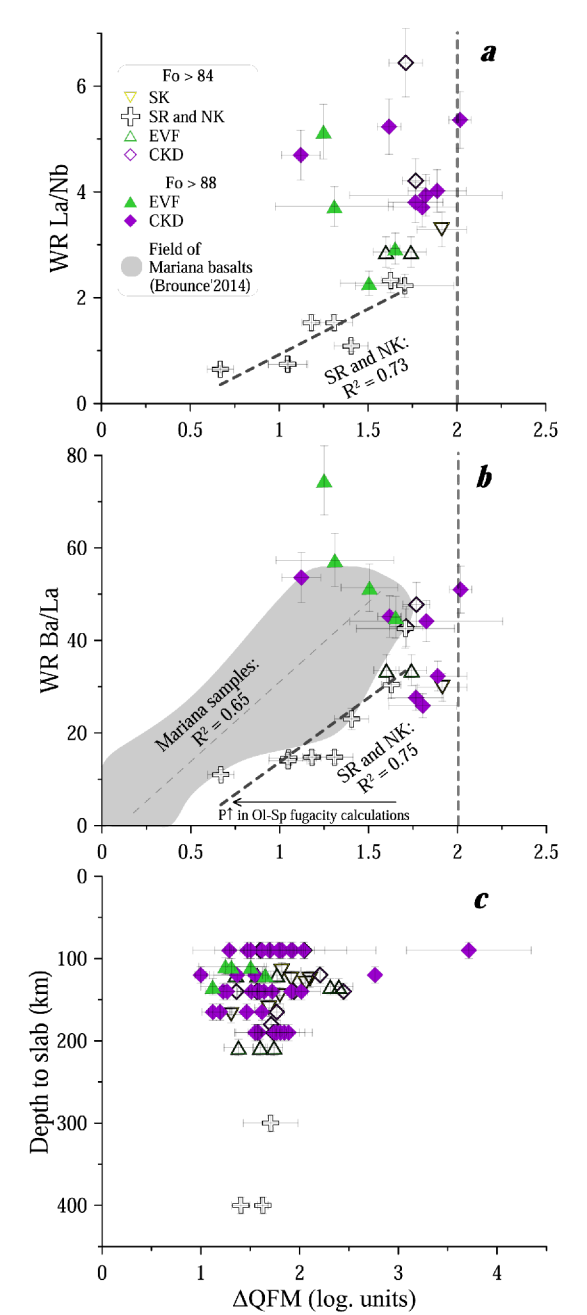
a
Fo > 84
SK
SR and NK
EVF
CKD
Fo > 88
EVF
CKD
Field of Mariana basalts (Brounce'2014)
SR and NK: R² = 0.73
WR La/Nb
b
Mariana samples: R² = 0.65
SR and NK: R² = 0.75
P↑ in Ol-Sp fugacity calculations
WR Ba/La
c
Depth to slab (km)
ΔQFM (log. units)

Figure 6

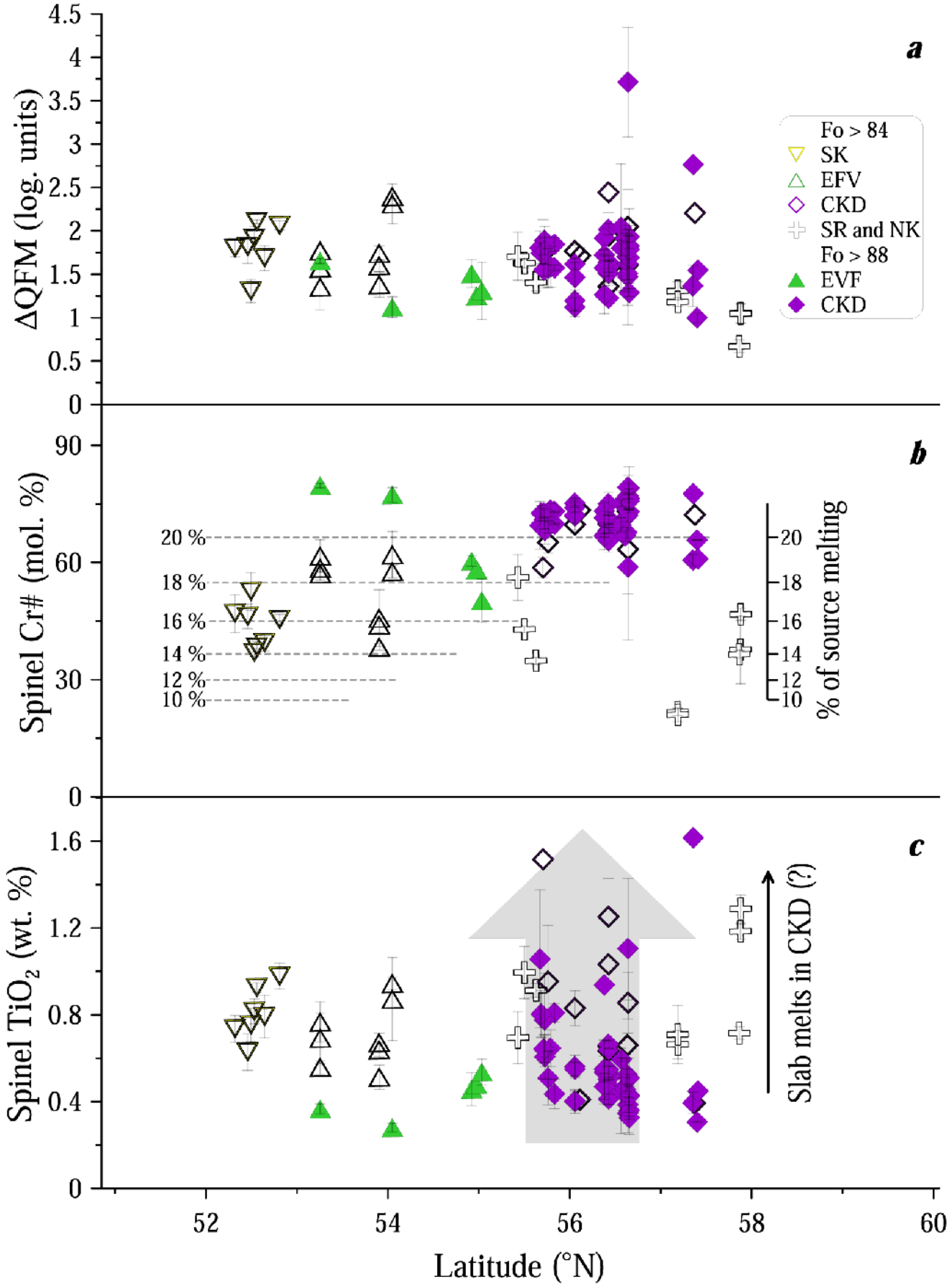
a
b
c
ΔQFM (log. units)
Spinel Cr# (mol. %)
Spinel TiO2 (wt. %)
Latitude (°N)
% of source melting
Slab melts in CKD (?)
Fo > 84
SK
EFV
CKD
SR and NK
Fo > 88
EVF
CKD
20 %
18 %
16 %
14 %
12 %
10 %

Figure 7

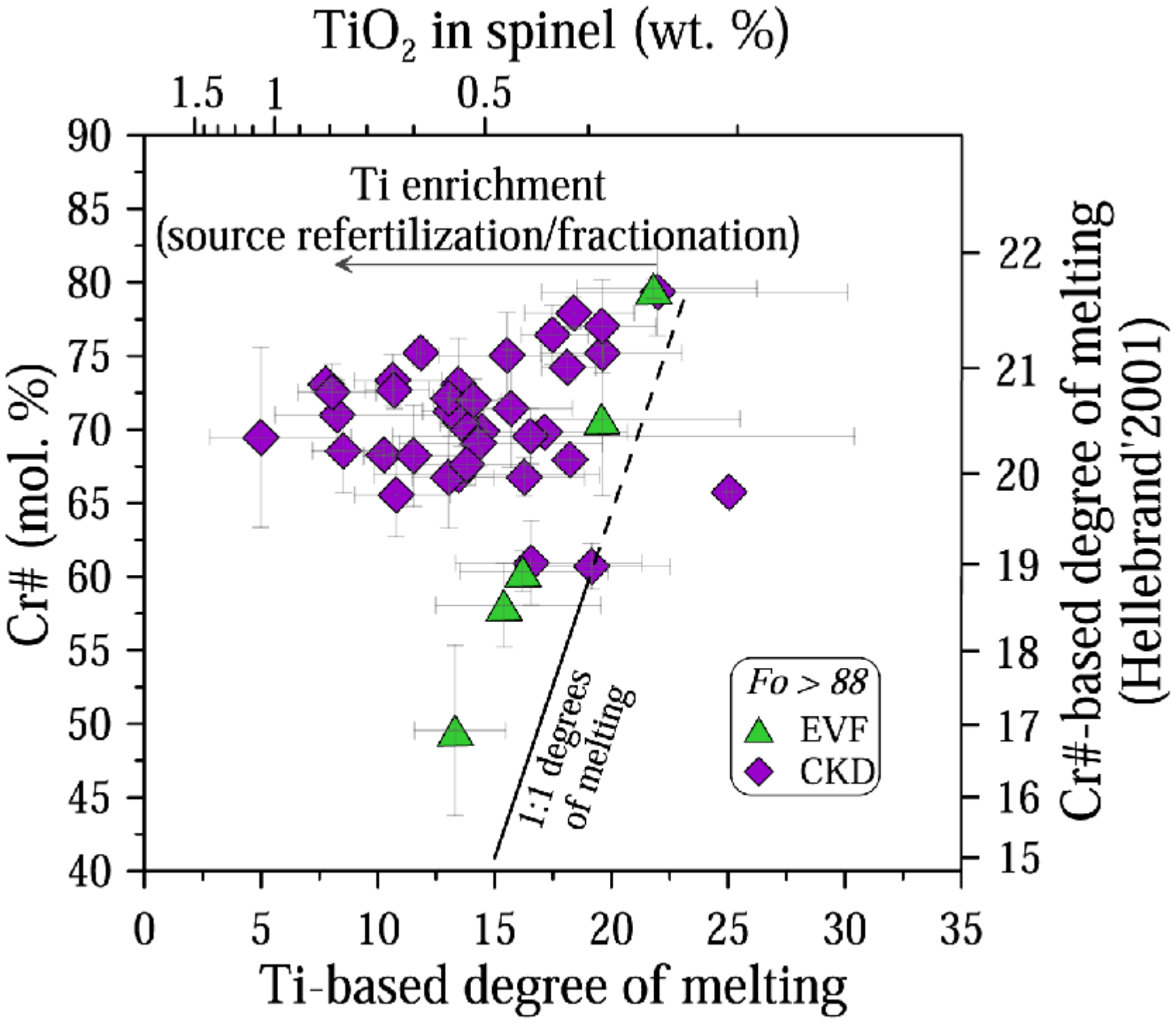
TiO2 in spinel (wt. %)
1.5
1
0.5
Ti enrichment
(source refertilization/fractionation)
Cr# (mol. %)
Cr#-based degree of melting
(Hellebrand'2001)
Ti-based degree of melting
1:1 degrees of melting
Fo > 88
EVF
CKD

Figure 8